Incremental Transient Energy-Based Directional Comparison Protection Scheme using IEC-61869-9 Sampled-Values

A. C. Adewole, A. Rajapakse, D. Ouellette, P. Forsyth

***Abstract*—Overcurrent protective relays are often applied as backup protection on transmission lines. However, they could wrongly operate for remote faults in some cases. One way of mitigating this is by using directional comparison schemes. This paper presents a directional comparison scheme based on a new Incremental Transient Energy (ITE)-based overcurrent directional algorithm calculated using the interphase (differential) ITE derived from IEC 61869-9 sampled values of currents and voltages. The performance of the proposed ITE algorithm was tested in a Directional Comparison Blocking (DCB) scheme between two substations. Performance evaluation was carried out using the IEEE EMTP reference test system for protective relay testing modelled in the RSCAD software, and several scenarios were carried out using a real-time simulation platform. The results obtained demonstrate the effectiveness of the proposed scheme.**

***Keywords*: Directional algorithm, directional comparison scheme, IEC 61969-9, incremental quantities, overcurrent protection, sampled values, transient energy.**

I. Introduction

DIRECTIONAL comparison schemes have always played a role in the timely clearance of transmission lines by responding to faults in a protection zone without any time delay. This is commonly used to provide high-speed relaying and also minimize the misoperation of the overreaching element of distance or overcurrent protective relays during reverse faults.

The traditional directional comparison scheme is based on pilot communication using microwave, radio, and telephony to send blocking or permissive trip signals to distance or overcurrent relays during reverse faults. Such schemes require directional elements to correctly identify the fault direction (forward or reverse) from the relaying point or zone of protection. Several algorithms for directionality exist in the literature, and the theory behind the most commonly used approaches based on phase and sequence components of faults can be found in [1-2].

In [1], the phase relationship between the positive sequence voltage and current fault signals were used in the design of a directional algorithm. Protection schemes based on the relative changes in the travelling waves of currents and voltages were described in [3]-[7]. Also, a transient directional protection technique based on wavelet transform was presented in [8]. Similarly, approaches based on the polarity of high frequency transient currents generated during faults were described in [9], [10].

Furthermore, techniques based on incremental (superimposed) quantities obtained as deviations between steady-state and fault voltage or current signals were presented in [11]-[19].

This paper extends the method in [11], [17] by exploring the application of incremental transient energy calculated using differential (interphase) voltages and currents, and measurements based on the IEC 61869-9 Sampled Values (SVs), and is applied to a communication-based transmission line directional comparison scheme.

The main contributions of this paper can be summarized as follows: (i) the application of the superposition principles in the development of a new incremental quantities-based directional algorithm using differential (interphase) Incremental Transient Energy (ITE), (ii) the design of a high-speed directional comparison scheme based on IEC 61869-9 SVs, (iii) real-time testing of the proposed algorithm and scheme using a co-simulation Real-Time System (RTS) platform.

The remainder of the paper is organized as follows. Section II describes the proposed directional detection algorithm, while Section III presents its application in a directional comparison scheme. Section IV presents and discusses the results obtained, while Section V summarizes the contribution of the paper.

II. Proposed Directional Detection Algorithm

This section describes the theoretical principle behind incremental quantities in power systems and the formulation of the ITE algorithm.

A. Basic Principles of Incremental Quantities

Faults in power systems would cause the currents and voltages at the relaying point to deviate from their prefault quantities. If the superposition principle is applied to the multi-source circuit shown in Fig. 1(a), the changes in the voltage or current signals at the relaying point can be calculated by removing all the prefault voltage sources and representing the network components with their impedances as shown in Fig. 1(b).

The superimposed quantities can be considered to be

This work was supported in part by RTDS Technologies Inc. Canada and Mitacs Accelerate Program, Canada.

A.C. Adewole and A. Rajapakse are with the University of Manitoba, Winnipeg R3T5V6 Canada (e-mail of corresponding author: adeyemi.adewole@umanitoba.ca). D. Ouellete and P. Forsyth are with RTDS Technologies Inc. Winnipeg R3T 2E1 Canada.

Paper submitted to the International Conference on Power Systems Transients (IPST2019) in Perpignan, France June 17-20, 2019

generated by a fictitious driving voltage source ($-\Delta v_F$) at the fault location, with a voltage equal in magnitude and phase to the prefault voltage at the fault point.

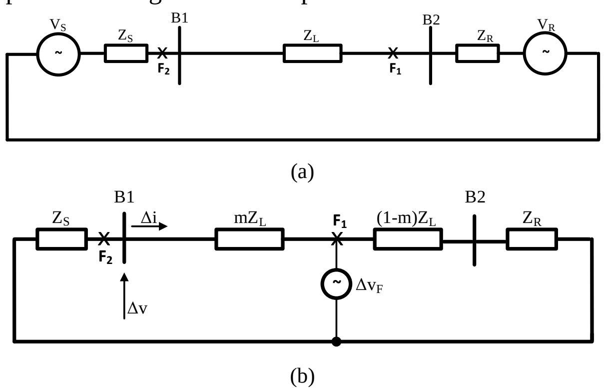

Fig. 1. Two-source transmission system (a) steady-state network, (b) superimposed network for a forward fault on the line between Buses B1 and B2

The voltage (v^{fault}) and current (i^{fault}) during the fault are given as:

$$v^{fault}(t) = v^{pre}(t) + \Delta v(t) \quad (1)$$

$$i^{fault}(t) = i^{pre}(t) + \Delta i(t) \quad (2)$$

where v^{pre} and i^{pre} are the prefault voltage and current quantities, Δv is the superimposed (incremental) voltage, and Δi is the superimposed current.

From Fig. 1(a), the voltage at the relaying point for a forward fault (F_1) is given by:

$$\Delta v(t) = -|Z_S| \cdot \Delta i(t) \quad (3)$$

The voltage for a reverse fault at (F_2) is given as:

$$\Delta v(t) = |Z_L + Z_R| \cdot \Delta i(t) \quad (4)$$

where Z_S, Z_R, Z_L are the impedances of the local source S, the remote source R, and the line, respectively.

B. Proposed Incremental Transient Energy Directional Algorithm

The incremental transient energy (e_{inc}) in a system is the integral of the product of the incremental voltage and current quantities:

This is given by:

$$e_{inc}(t) = \int_0^T \Delta v(t) \cdot \Delta i \, dt \quad (5)$$

From Fig. 1(a), it can be inferred that the transient energy $e_{inc,fwd}$ for a forward fault is related to the energy absorbed e^{fault} by the equivalent impedance during the fault.

$$e_{inc,fwd}(t) = -e^{fault}(t) \quad (6)$$

Similarly, the incremental transient energy ($e_{inc,rvs}$) for a reverse fault is given as:

$$e_{inc,rvs}(t) = e_L(t) + e_R(t) \quad (7)$$

where e_L and e_R are the energies absorbed during the fault by the line and remote source impedances, respectively.

During normal operating condition, the incremental transient energy is zero. This changes to a nonzero value during faults.

The differential (interphase) incremental transient energy can be expressed as:

$$e_{inc,AB}(t) = \int_0^T \Delta v_{AB}(t) \cdot \Delta i_{AB} \, dt \quad (8)$$

$$e_{inc,CA}(t) = \int_0^T \Delta v_{CA}(t) \cdot \Delta i_{CA} \, dt \quad (9)$$

where $e_{inc,AB}$, Δv_{AB}, and Δi_{AB} are the differential incremental energy transient, incremental voltage, incremental currents between phases A and B. $e_{inc,CA}$, Δv_{CA}, and Δi_{CA} are the differential incremental energy transient, incremental voltage, incremental currents between phases C and A.

$$\Delta i_{AB} = \left(i_A^{fault} - i_B^{fault}\right) - \left(i_A^{pre} - i_B^{pre}\right) \quad (10)$$

$$\Delta v_{AB} = \left(v_A^{fault} - v_B^{fault}\right) - \left(v_A^{pre} - v_B^{pre}\right) \quad (11)$$

Similar derivation applies for the differential quantities for phase CA.

From (6) and (7), it can be seen that the incremental transient energy at the relaying point is negative for a forward fault and positive for a reverse fault. Based on the above, the polarity of the incremental transient energy can be applied for directional protection as follows:

$$e_{inc} < 0 \text{ for a forward fault} \quad (12)$$

$$e_{inc} > 0 \text{ for a reverse fault} \quad (13)$$

The flowchart for the proposed ITE algorithm is shown in Fig. 2. The process starts with the acquisition of the IEC 61869-9 SVs of currents and voltages published by merging units. The 96 samples per cycle of SVs are downsampled to 8 samples per cycle and stored in a 3-cycles buffer. When a fault is detected and the incremental quantities threshold alarms are triggered, the incremental transient energy is calculated, and its polarity is used in identifying the fault direction.

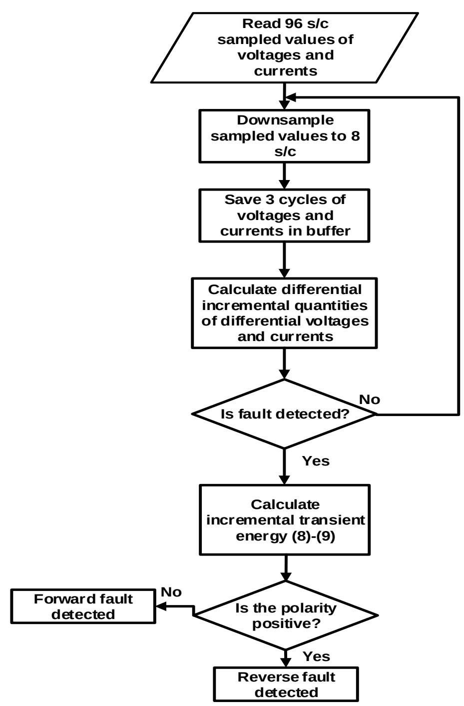

Fig. 2. Proposed incremental transient energy directional algorithm

III. Directional Comparison Scheme

Directional Comparison Blocking (DCB) schemes provide high-speed fault clearance for internal faults occurring on a protected line provided a blocking signal is not received from the remote end. It requires a directional algorithm capable of identifying if a fault is internal to the protection zone or otherwise. DCB schemes can be based on distance or overcurrent protective elements. This section describes the overcurrent-based DCB scheme implemented in this paper using the proposed ITE directional algorithm.

For an internal fault, the fault direction is inward at the line terminals from the buses at both ends, while for an external fault, the fault direction will be outward at one of the buses and inward at the other bus. For example, when an external fault at a remote end occurs, one of the protective relays (e.g at a local Bus – Bus 1) will detect a forward fault, while the other protective relay (at a remote Bus – Bus 2) will detect a reverse fault. In order to prevent the protective relay at Bus 1 from operating for a remote fault, the relay at Bus 2 will send a blocking signal to the relay at Bus 1.

The protection scheme logic that was implemented in this paper is shown in Fig. 3. The scheme is designed for instantaneous directional overcurrent tripping ($67PG_{ITE}$) for internal phase ($67P_{ITE}$) and ground ($67G_{ITE}$) faults occurring on a protected line using phase overcurrent (50P) and ground overcurrent (50G) elements, respectively. When the DCB scheme is enabled using the DCB key (shown in Fig. 3), a fault on the protected line will be seen by the protective relays at both ends ($67PG_{ITE1}$ and $67PG_{ITE2}$). If no blocking signal is received from the remote end, they will operate their respective breakers after the pre-programmed coordination time delay.

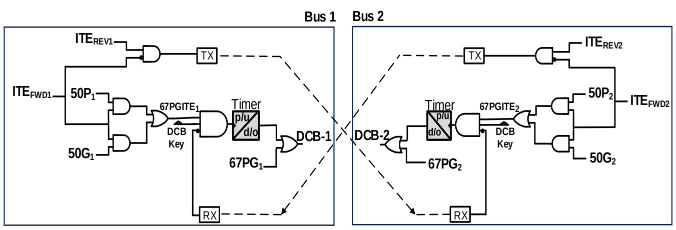

Fig. 3. Proposed DCB scheme using the proposed ITE algorithm

One particular advantage of the DCB scheme is that the speed of operation of the protective relays at the faulted section is consistent since it does not have to wait for any permissive logic. Also, it is simple, sensitive, and reliable. Furthermore, since only binary signals are exchanged between the remote ends, it does not require a high communication bandwidth.

IV. Experimental Results

This section presents the performance testing of the proposed algorithm using a RTS platform.

A. Test System Modelling

To validate the proposed ITE-based directional algorithm, the IEEE EMTP reference model for transmission line protective relaying testing [20] was modelled in the RSCAD software. The test system (Fig. 4) is a 345 kV network with three sources, and a parallel transmission line between Sources S1 and S2. A third line is tapped off the middle of the parallel transmission line, and has a normally-open switch SW. The test carried out in this paper were done with SW open, with an ITE-based directional overcurrent protection implemented at both ends of Line-1 (Bus 1 and Bus 2). The parameters of the various components in the test system can be found in [20].

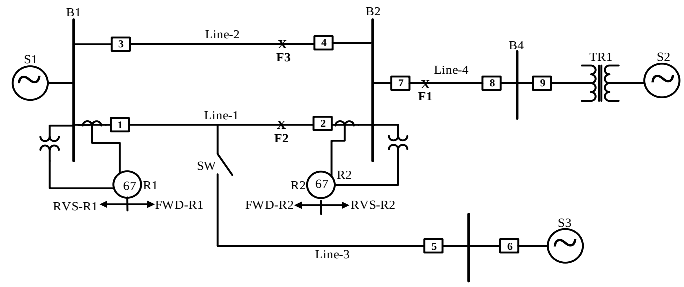

Fig. 4. IEEE EMTP reference model for transmission line relay testing [20]

B. Hardware-in-the-Loop Implementation

Fig. 5 shows the real-time simulation platform implemented for testing the proposed IEC 61869-9 SV-based DCB scheme using the proposed ITE directional algorithm. It comprises of two RTDS® racks with Rack-1 used in simulating the power system network, while Rack-2 serves as the protection platform for implementing the directional overcurrent-based DCB scheme. The three phase currents and voltages from the secondary terminals of the Current Transformers (CTs) and the Voltage Transformers (VTs) located at both ends of Line 1 are published as IEC 61869-9 SVs with a sampling rate of 96 samples per cycle using the GT-FPGA device (serving as a merging unit) connected to Rack-1. The SVs from Rack-1 are subscribed by Rack-2 using the GTNET-SV card. The subscribed SVs serve as the input to the DCB protection scheme.

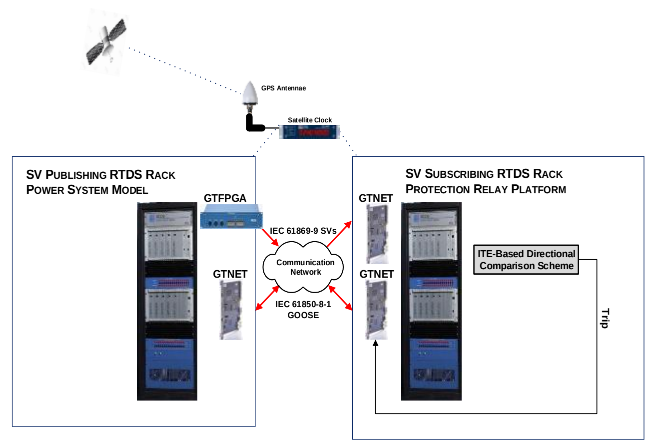

Fig. 5. Implemented real-time simulation platform

Two overcurrent elements (for phase and ground faults) supervised by the ITE algorithm were implemented at both ends of Line-1. The incremental quantities are computed using a 3-cycle buffer for storing the prefault quantities. Although, a 2-cycle buffer of prefault quantities will suffice, a 3-cycle buffer was used instead in order to obtain the exact multiples of SVs that correspond to the simulation time-step of 50 µs. The ITE-based directional algorithm is enabled when the Δi and Δv quantities exceed their pickup thresholds.

This is given as:

$$\Delta i \geq 0.2 I_{nom} \quad \text{AND} \quad \Delta v \geq 0.1 V_{nom} \tag{14}$$

where I_{nom} and V_{nom} are the nominal secondary CT current and secondary VT voltage, respectively.

The polarity of the incremental energy transient is determined using the samples in a quarter-cycle window.

C. Case Studies, Results and Discussions

Several scenarios consisting of various fault types, fault locations, fault resistances, and fault inception angles were carried out in order evaluate the performance of the proposed algorithm as given below.

Ground and Phase Faults: Fig. 6 shows the incremental currents and voltages for a reverse A-g fault with a fault resistance of 5 Ω and fault inception angle of 90° at 5% of Line-4 (F1). From Fig. 6(a), it can be seen that the currents at both ends of Line-1 are 180° out of phase, while the incremental voltages are shown in Fig. 6(b). Fig. 7 presents the incremental transient energy for an A-g forward (internal) fault at 90% of Line-1 (F2). For an internal fault, the currents at both ends are in phase. Thus, the polarity of the incremental energy (first half-cycle) at both ends will be positive. However, the incremental voltage will be negative. From Fig. 7, it can be seen that the first half-cycle polarity of the incremental transient energies at the relays located at Bus 1 and Bus 2 (End-1 and End-2) of Line-1 have a negative polarity. Thus, a forward fault is identified on the protected line.

Also, the two differential ITEs (AB and CA) detected the fault since the A-g fault affects the A-phase, and is common to both of them. Furthermore, high speed detection was achieved using a 4 ms window of the incremental transient energy.

When applied to a DCB scheme, no blocking signal will be issued since both ends would detect a forward fault. Thus, the ITE-based overcurrent relays ($67PG_{ITE}$) at both ends will operate correctly for the internal fault.

Fig. 8 shows the results for a close-in reverse (external) fault at 5% of the adjacent line (Line-4). The $67PG_{ITE}$ relay at Bus 1 would detect a forward fault (indicated by a negative incremental transient energy polarity), while the $67PG_{ITE}$ relay at Bus 2 would detect a reverse fault (indicated by a positive incremental transient energy polarity), and issue a carrier signal to Bus 1. The $67PG_{ITE}$ would operate after an intentional coordination time delay if the fault is still on the line.

Figs. 9-10 show the response obtained for BC and ABC reverse faults at 5% of Line-4. The results obtained were consistent with that presented for the A-g fault in Fig. 8. Also, the results at both ends of Line-1 for various fault resistances are shown in Fig. 11. Although the value of the ITE reduced significantly as the fault resistance increased, the ITE algorithm correctly indicated the fault direction for fault resistances up to 100 **Ω**. Furthermore, similar results were obtained for various fault inception angles (0°:30°:180°).

Fig. 12(a) shows the phase currents at Bus-1 and Bus-2, and the binary signals for an internal Ag fault with 5 **Ω** fault resistance, 0° fault inception angle at 5% of Line-1. The directional algorithms (67PGITE1 and 67PGITE2) and the DCBs (DCB-1 and DCB-2) at both end correctly indicated a forward (internal) fault, and trip signals were issued to open the circuit breakers at both ends. Similarly, Fig. 12(b) shows the results for an external Ag fault at 20% of Line-4 with a 5 **Ω** fault resistance and 0° fault inception angle. It can be seen that the 67PGITE1 signal correctly indicated a forward fault. However, a block signal was received from the remote end. Thus, the DCB-1 signal is low. Also, the 67PGITE2 and DCB-2 are low indicating a reverse fault. Therefore, the DCB scheme did not issue any trip signal as expected.

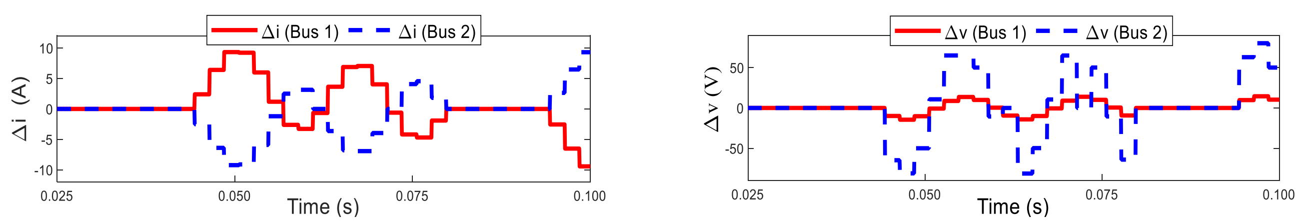

(a) (b)

Fig. 6. Incremental quantities at Buses B1 and B2 for an A-g reverse fault on Line-4 (a) incremental currents and (b) incremental voltages

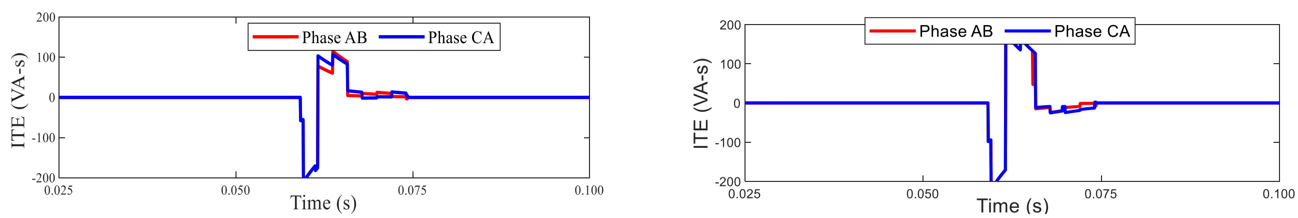

(a) (b)

Fig. 7. Incremental transient energy for A-g internal fault on Line-1 (a) ITE at End-1 and (b) ITE at End-2

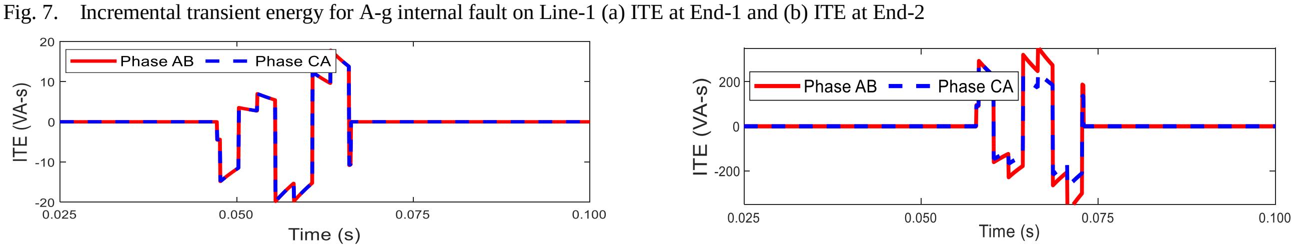

(a) (b)

Fig. 8. Incremental transient energy for A-g external fault on Line-4 (a) ITE at End-1 and (b) ITE at End-2

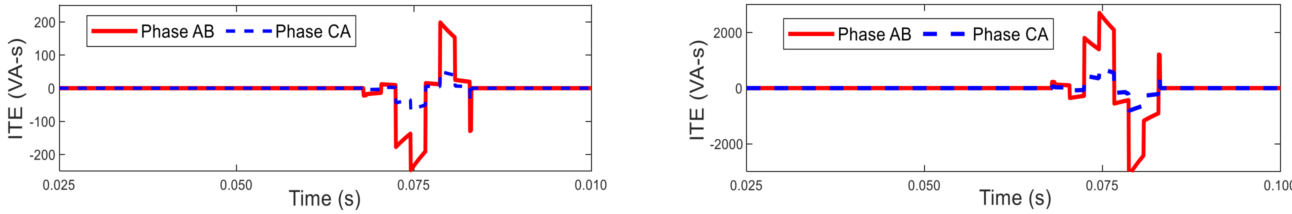

(a) (b)

Fig. 9. Incremental transient energy for BC external fault on Line-4 (a) ITE at End-1 and (b) ITE at End-2

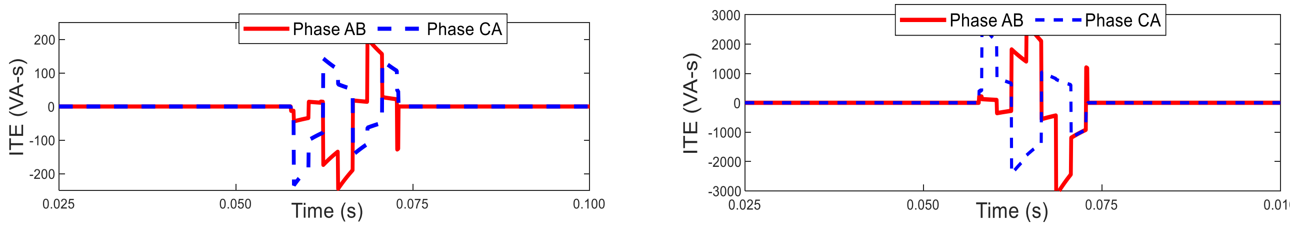

(a) (b)

Fig. 10. Incremental transient energy for ABC external fault on Line-4 (a) ITE at End-1 and (b) ITE at End-2

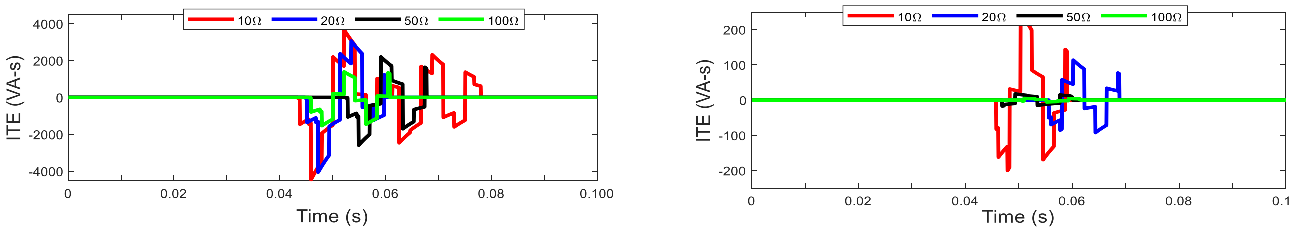

(a) (b)

Fig. 11. Incremental transient energy for A-g internal faults on Line-1 for various fault resistances (a) ITE at End-1 and (b) ITE at End-2

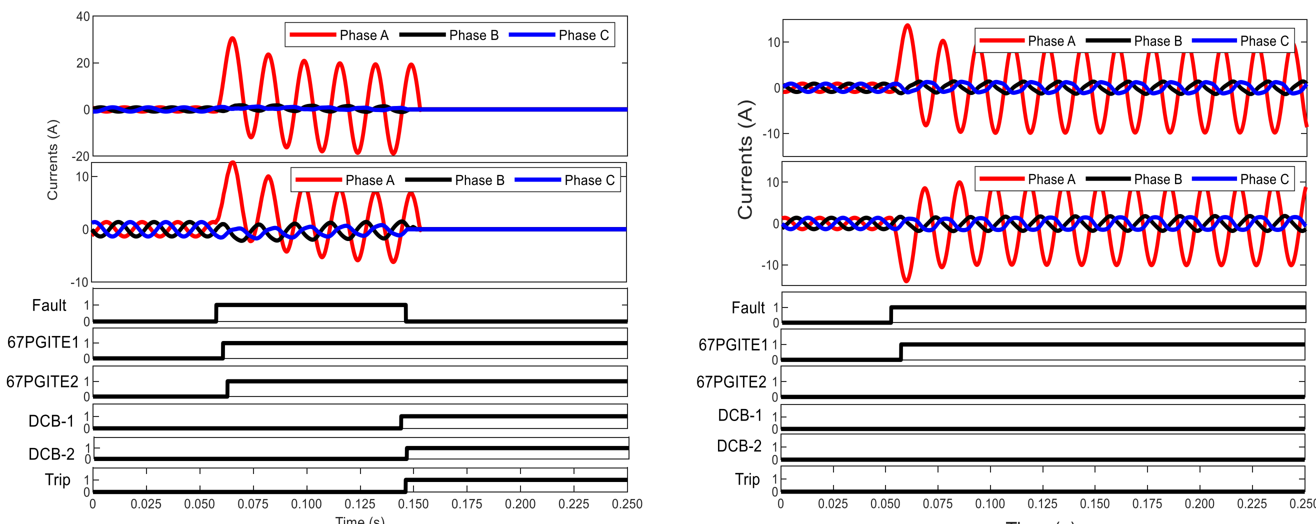

(a) (b)

Fig. 12. Phase currents and binary signals for the DCB scheme (a) A-g internal fault and (b) A-g external fault

Effects of Mutual Coupling: Mutual coupling between two or more transmission lines in parallel could cause zero sequence currents to flow in the unfaulted parallel transmission line because of the magnetic fields between these parallel lines. This could cause an overcurrent protection relay to wrongly operate for ground faults on the adjacent line. Fig. 13 shows the results obtained for a line-end (F3) A-g fault on the adjacent parallel line (90% of Line-2) with the circuit breakers at both ends closed. The $67PG_{ITE}$ at both ends correctly indicated a reverse fault as shown by the positive ITE polarity at both ends of the line.

A peculiar case of current reversal could occur if a fault occurs on an adjacent transmission line with one of its circuit breakers open. An A-g fault at 90% of Line-2 with an open circuit breaker at Bus B2 on Line-2 will result in a current reversal, causing the fault currents to flow from Line-2 to Line-1 through Bus B1. From Fig. 14, it can be seen that a reverse fault was correctly indicated by Line-1 $67PG_{ITE1}$ protective relay at Bus 1, while a forward fault was seen by the $67PG_{ITE2}$ protective relay at the other end (B2).

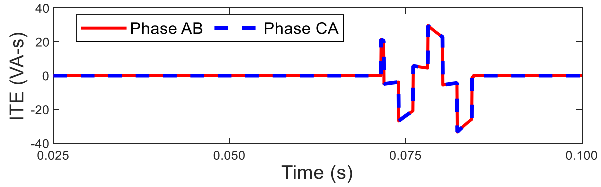

(a)

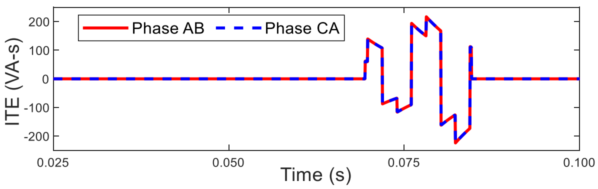

(b)

Fig. 13. A-g fault on parallel line (Line-2) with all circuit breakers closed (a) ITE at Bus 1 of Line-1 and (b) ITE at Bus 2 of Line-1

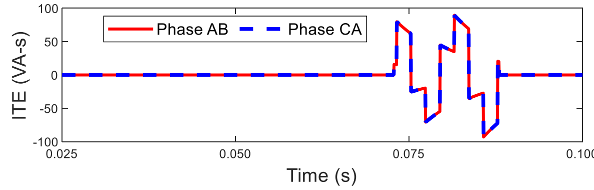

(a)

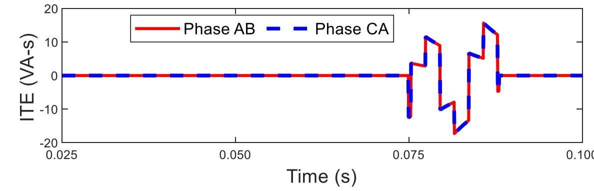

(b)

Fig. 14. A-g fault on parallel line (Line-2) with remote circuit breaker open at Bus 2 of Line-2 (a) ITE at Bus 1 of Line-1 and (b) ITE at Bus 2 of Line-1

V. Conclusions

This paper proposed a new IEC 61869-9 SV-based incremental energy-transient algorithm that was applied in a directional comparison scheme, and tested using a real-time HIL simulation platform.

Several tests using real-time simulations were carried out for various fault types, fault resistances, fault inception angles, and fault locations. Also, the impact of zero sequence mutual coupling on the ITE-based algorithm was investigated. A quarter-cycle operating time was established for the ITE-based directional algorithm. Furthermore, a DCB scheme using the proposed ITE-based directional algorithm was implemented and tested. The ITE-based directional algorithm and DCB scheme showed high reliability for the various fault conditions considered.

VI. References

[1] H. Gao and P. A. Crossley, 'Design and evaluation of a directional algorithm for transmission line protection based on positive-sequence fault components', *IET Gener. Transm. Distrib*., 2006, vol 153, iss. 6, pp. 711–718, 2006.

[2] E. O. Schweitzer and J. Robert, "Distance relay element design," *SEL Journal of Reliable Power*, vol. 1, no. 1, pp. 1-28, 2010.

[3] S. Bin, D. Xinzhou, S. Yuanzhang, Z. Q. Bo, and H. Jiali, "New principle of high-speed directional relay," in *Proc. Power Eng. Soc. Summer Meeting*, 2002, vol. 1, pp. 387–392.

[4] J. Zhao, Y. Chen, and P. Crossley, "Design and evaluation of a directional relay for use within a distribution network restoration scheme," in *Proc. Power Eng. Soc.Winter Meeting*, 2000, vol. 4, pp. 2374–2378.

[5] M. M. Eissa and O. P. Malik, "A new digital directional transverse differential current protection technique," *IEEE Trans. Power Del.*, vol. 11, no. 3, pp. 1285–1291, Jul. 1996.

[6] K. S. Prakash, O. P. Malik, and G. S. Hope, "Amplitude comparator based algorithm for directional comparison protection of transmission lines," *IEEE Trans. Power Del*., vol. 4, no. 4, pp. 2032–2041, Oct. 1989.

[7] J. He, Y. Zhan, and N. Yan, "New type power line carrier relaying system with directional comparison for EHV transmission lines," *IEEE Trans. Power App. Syst.*, vol. PAS-97, no. 3, pp. 429–436, Mar. 1984.

[8] W. Chan, O. P. Malik, X. Yin, D. Chen, and Z. Zhang, "Study of wavelet based ultra high speed directional transmission line protection," *IEEE Trans. Power Del.*, vol. 18, no. 4, pp. 1317-1322, Oct. 2003.

[9] A. Pathirana, A. Rajapakse, and N. Perera, "Development of a hybrid protection scheme for active distribution systems using polarities of current transients," *Electric Power Systems Research*, vol. 152, pp. 377–389, Nov. 2017.

[10] Z.Q. Bo, X.Z. Dong, B.R.J. Caunce, J.H. He, D. Thomolier, A Klimek, Z. Chen, and M.A. Redfern, "Application of transient polarity comparison technique to power system protection," *IEEE PES Transmission and Distribution Conference and Exhibition: Asia and Pacifi*c, Dalian China, pp. 1-6, 2005.

[11] Y. Kong, B. Zhang, and Z. Hao, "Study of ultra-high-speed protection of transmission lines using a directional comparison scheme of transient energy, *IEEE Trans. Power Delivery*, vol. 30, pp. 549-557, Jun. 2015.

[12] B. Gu, J. Tan, and H. Wei, "High speed directional relaying algorithm based on the fudamental frequency positive sequence superimposed components," *IET Gener. Transm. Distrib.*, vol. 8, iss. 7, pp, 1211-1220, Dec 2013.

[13] S. M. Hashemi, M. Tarafdar Hagh, and H. Seyedi, "High-speed superimposed-based protection of series-compensated transmission-line protection: A directional comparison scheme using the average of superimposed components" *IEEE Trans. Power Del*., vol. 28, no. 2, pp. 955-964, Apr. 2013.

[14] P. Jafarian and M. Sanaye-Pasand, "High-speed superimposed-based protection of series-compensated transmission lines*," IET Gener. Transm. Distrib*., vol. 5, iss. 12, pp. 1290-1300, Apr. 2011.

[15] C. Aguilera, E. Orduna, and G. Ratta, 'Directional traveling-wave protection based on slope change analysis', *IEEE Trans. Power Del*., vol. 22, iss. 4, pp. 2025–2033, 2007.

[16] G. Benmouyal and J. Mahseredjian, "A combined directional and faulted phase selector element based on incremental quantities," *IEEE Trans. Power Del*., vol. 16, no. 4, pp. 478–484, Oct. 2001.

[17] P. Apostolov, D. Tholomier, and S. H. Richards, "Superimposed components based sub-cycle protection of transmission lines," *in Proc. IEEE Power Eng. Soc. Power Syst. Conf. Expo*., New York, pp. 592–597, 2004.

[18] P. G. McLaren, G. W. Swift, Z. Zhang, E. Dirks, R. P. Jayasinghe, and I. Fernando, "A new directional element for numerical distance relays," *IEEE Trans. Power Del.*, vol. 10, no. 2, pp. 666–675, Apr. 1995.

[19] T. Johns, "New ultra high speed directional comparison technique for the protection of EHV transmission lines," *Proc. Inst. Elect. Eng., Gen., Transm. Distrib.*, vol. 127, pp. 228–239, 1980.

[20] Power Syst. Relaying Comm., "EMTP reference models for transmission line relay testing," Final, Tech. Rep., 2005. [Online]. Available: www.pes-psrc.org.